Capacity of Measured MIMO Channels in Dependence of Array Element Spacing and Distance between Antennas

D. Yacoub *, C. Schneider †, S. Warzuegel ‡, W. G. Teich *, R. Thomä †, J. Lindner*
* University of Ulm, Department of Information Technology, Ulm, Germany
Email: {doris.yacoub, werner.teich, juergen.lindner}@uni-ulm.de
† University of Ilmenau, Dept. of Electrical Engineering and Information Technology, Ilmenau, Germany
Email: {Christian.Schneider, Reiner.Thomae}@tu-ilmenau.de
‡ MEDAV GmbH, Uttenreuth, Germany
Email: steffen.warzuegel@medav.de

***Abstract*— In this paper, we investigate the effect of antenna spacing within the transmitter and receiver arrays as well as the distance between the transmitter and receiver arrays on the capacity of a measured multiple-input multiple-output (MIMO) channel. During the measurement, the transmitter was mounted on a vehicle moving at a constant speed towards the receiver which was mounted on a bridge. The capacity, as expected, was found to increase with increased antenna element spacing within the transmitter or receiver arrays. However, the resulting capacity curves versus distance were found to fluctuate as the transmitter approached the receiver. Reflections from the street surface are assumed to be the cause of those fluctuations. In order to test this theory, we simulated a simple two-path channel model.**

I. Introduction

In the last few years, the need for reliable transmission at high rates has shifted the attention towards multiple-input multiple-output (MIMO) systems. The capacities of MIMO channels have been calculated for Rayleigh fading channel models (e. g. [1]) as well as for frequency selective channel models (e. g. [2]). In this paper, we look at the capacity of a real measured channel with a strong line of sight (LOS) component and investigate the effect of array element spacing and the seperation between the transmitter and receiver arrays on the MIMO channel capacity. The transmitter was mounted on a vehicle moving at a low speed towards the receiver, which was mounted on a bridge. The channel was measured for several transmitter as well as receiver array element spacings and was continuously measured as the transmitter approached the receiver. The results have shown that despite the strong LOS component, the capacity was found to fluctuate in a periodic manner as the vehicle moved. Reflections from the street surface are assumed to be responsible for such an effect. To test this assumption, a simple two-path model was simulated and compared to the measured channels.

Throughout this paper, vectors and matrices will be denoted by underlined and doubly-underlined letters, respectively. Lowercase letters will be used for the time domain whereas the uppercase letters for the frequency domain. Scalars will be simply designated by letters.

II. Measurment Setup

In this section, we briefly describe the measurement setup at both the transmitter and the receiver. The transmitter (Tx) was mounted on a vehicle moving at a constant low speed (around 10 km/h, doppler shift thus neglected) towards a stationary receiver (Rx), which was mounted on a bridge (Fig. 1). The channel measurements were started as the vehicle was about 217 m in front of the bridge and stopped after it passed the bridge by around 62 m (Fig. 1). The channel measurements were carried at a center frequency, f_o, of 5.2 GHz and for a bandwidth, BW, of 120 MHz. For more details about channel sounder measurements, please refer to [3]. The transmitter and receiver array setups are shown in Fig. 2. The receive elements were tilted down by 45^o. The MIMO channel was measured for three different setups at the receiver and two setups at the transmitter. The setups correspond to different antenna element spacings within either the transmitter or receiver arrays. The total span, W, and separation between the antennas, d (also given as a function of the wavelength, $\lambda = 0.0577$ m), for the three setups at the receiver are given in the following table.

Receiver Setup	W[m]	d[m]
Large (L)	17.5	$2.5 \approx 43\lambda$
Medium (M)	6.16	$0.88 \approx 15\lambda$
Small (S)	1.022	$0.146 \approx 2.5\lambda$

At the transmitter, the distances d_1 and d_2 for the two different setups are as follows:

Transmitter Setup	d_1[m]	d_2[m]
Large (L)	$0.862 \approx 15\lambda$	$0.944 \approx 16\lambda$
Small (S)	$0.185 \approx 3\lambda$	$0.185 \approx 3\lambda$

All combinations of the transmitter and receiver setups (6 in total) were used for channel measurement as well as for the capacity calculations. In all what follows, we shall denote the setups by the receiver setup (L, M or S) followed by the transmitter setup (L or S). For example, LS denotes the results of the MIMO channel measured using large receive and small transmit array element spacings.

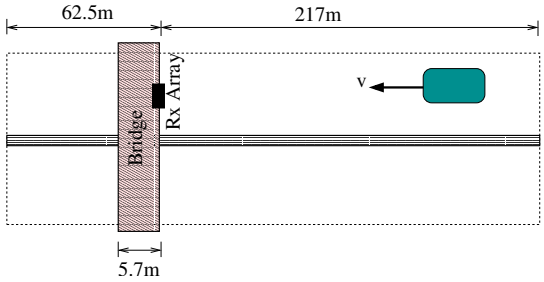

Fig. 1. Schematic of measurement setup.

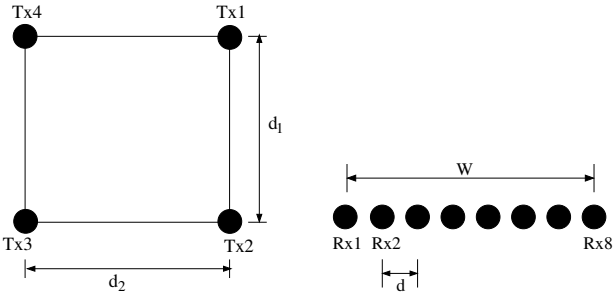

Fig. 2. Transmitter (left) and receiver (right) array setups.

III. MIMO Channel Capacity

The capacity of any channel can either be calculated in the frequency or the time domain. However, for a frequency selective channel, it is easier to calculate the capacity in the frequency domain. Assuming full channel knowledge at the receiver, the capacity, C_R, of a frequency selective channel can be calculated, for n_R receive antennas and n_T transmit antennas, as follows [2]:

$$C_R = \frac{1}{N}\sum_{n=1}^{N} log_2\{\det(\underline{\underline{I}}_{n_R} + \frac{\rho}{n_T}\underline{\underline{H}}_f(n)\underline{\underline{H}}_f^H(n))\}, \quad (1)$$

where $\underline{\underline{H}}_f(n)$ is a matrix of size $n_R \times n_T$ and represents the channel transfer function at frequency n for $n = 1, \ldots, N$ frequencies and ρ is the signal to noise ratio (SNR). The capacity can also be calculated from the eigenvalues, Λ_i, of $\underline{\underline{H}}_f(n)\underline{\underline{H}}_f^H(n)$ for $n = 1, \ldots, N$ as follows [2]

$$C_R = \frac{1}{N}\sum_{i=1}^{min(Nn_R, Nn_T)} log_2(1 + \frac{\rho}{n_T}\Lambda_i). \quad (2)$$

For capacity calculations of random channels, the channel is normalized such that $\mathcal{E}\{|\underline{h}(l)_{ij}|^2\} = 1$, where $\underline{h}_{ij}(l)$ are the channel impulse responses of the MIMO channel in the time domain between transmit antenna j ($j = 1, \ldots, n_T$) and receive antenna i ($i = 1, \ldots, n_R$) having $l = 1, \ldots, L$ taps.

A. Maximum Capacity in a Line of Sight Environment

In [4], it was shown that in a pure line of sight (LOS) environment (i. e. no scattering, $L = 1$), there exists a range between the transmitter and receiver arrays where the channel matrix is orthogonal (i. e. $\underline{\underline{H}}_f(n)\underline{\underline{H}}_f^H(n) = \underline{\underline{I}}_{n_R}$ and all eigenvalues are equal). This range contains all distances below D_{orth}, which is given by:

$$D_{orth} = \frac{d_{Tx} d_{Rx} n_R}{\lambda}, \quad (3)$$

where d_{Tx} is the spacing between the antenna elements in the transmitter, d_{Rx} the spacing between the antenna elements in the receiver and λ is the wavelength. Note that eqn. 3 only considers the orthogonality of the signatures for a pair of adjacent transmit antennas [4]. That is, it considers the orthogonality of the vectors $\underline{h}_k$ and $\underline{h}_{k+1}$, where $\underline{h}_k$ is the kth column of the $n_R \times n_T$ channel matrix, $\underline{\underline{h}}$, in the time domain. Similar results were also found in [5], where the channel capacity for a simulated 3×3 MIMO LOS channel was found to increase as the transmitter approached the receiver reaching its maximum value at the distance given by eqn. 3.

IV. Capacity of Measured MIMO Channels

All capacity calculations were done in the frequency domain for a bandwidth of 20MHz and $N = 256$, where N is the number of subcarriers, and were plotted versus the distance between the transmitter and receiver arrays. The receiver (bridge) is located at distance 0. Positive distances represent distances during which the transmitter (vehicle) is approaching the bridge, while negative ones represent those during which the vehicle is moving away from bridge. For the capacity calculations, the eigenvalues were normalized such that

$$\sum_{i=1}^{min(Nn_R, Nn_T)} \Lambda_i = n_T n_R N. \quad (4)$$

This, on the average, is equivalent to $\mathcal{E}\{|\underline{h}(l)_{ij}|^2\} = 1$. The capacity was calculated for $\rho = 20$ dB. The channel measurments were done using all four transmit and eight receive antennas. Yet, for the calculations either all channels or a subset of them were used for the capacity calculations. That way we could examine the effect of the number of transmit or receive antennas as well as the element spacing within either the transmittter or the receiver on the capacity. The antennas (see Fig.2) corresponding to the different channels used for the capacity calculations are given in the following table.

MIMO	2×2	2×4	2×8	4×4	4×8
Tx	1,3	1,3	1,3	1-4	1-4
Rx	1,8	1,3,5,7	1-8	1,3,5,7	1-8

For example, in case of MIMO 2×2, the channels corresponding to transmit antennas 1 and 3 and receive antennas 1 and 8 were used to calculate the capacity. Figure 3 shows the impulse response of a typical measured channel (absolute time versus delay). It is clear that the channel has a strong LOS component. Figures 4 and 5 show how the capacity changes with distance to bridge for the Large-Large (LL) and Small-Small (SS) array setups and different number of transmit and receive antennas. The dashed horizontal lines represent the maximum capacity that can be achieved for the given MIMO system (Sec. III-A). The numbers on the lines are the difference between the mean capacity over distance and the maximum one. As expected,

the capacity increases as the number of either transmit or receive antennas is increased. Also, as the number of receive antennas increases, the gap between the measured capacity and the maximum one decreases. Despite the strong LOS component, there was a minor change in the capacity as the transmitter approached the receiver. The capacity tends to increase with decreasing distance between the transmitter and receiver arrays, yet this change is very small and is most obvious in the LL setup than in any of the other setups (not shown here). The results contrast to what was expected in Sec. III-A. It can also be seen that the capacity fluctuates throughout the measurement distance. This is probably due to the reflections from the street surface that lead to either destructive of constructive intereference as the vehicle moves. To test this theory, the LOS model was extended to a two-path model. The results of the simulations will be shown in Sec. V. Figures 6 and 7 show the mean capacity over distance for all array spacing combinations. The solid lines represent the change in the mean capacity with increasing array spacing at the receiver and large array spacing at the transmitter (SL, ML, LL). The dashed one represents the change in the mean capacity for the small array spacing at the transmitter (SS, MS, LS). As expected, the larger the spacing between the antennas within either the transmit or receive arrays, the higher the capacity. The MIMO $2 \times n_R$ capacity does not always confirm to this expection. This maybe due to the fact that we have chosen antennas elements that are furthest away from each other, and thus the effect of the antenna spacing is not as strong especially for the 2×2 system. Also note that the large antenna seperation at the transmitter is almost equal to the medium one at the receiver. The mean capacities for SL and MS setups are thus, as expected, almost equal (Figs. 6 and 7).

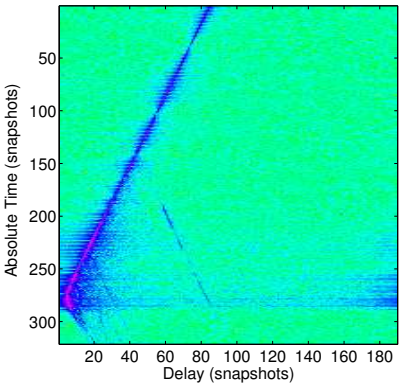

Fig. 3. Channel impulse response of typical measured channel.

V. Two Path Channel Model

In this section, we model the measured channel between **one** pair of antennas elements using a two-path geometrical channel model with delay difference, $\Delta\tau = \tau_2 - \tau_1$. The delays are given by, $\tau_i = \frac{d_i}{c}$, for $i = 1, 2$, where d_i is the distance traveled by the signal over the ith path. We have assumed no doppler shift, i. e. $f_d = 0$. The first path is a line of sight (LOS) path. The second path is assumed to occur due to reflections

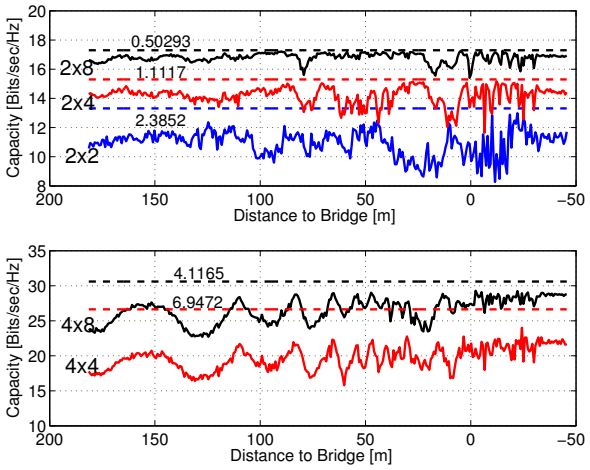

Fig. 4. Capacity versus distance for Large-Large (LL) setup, $\rho = 20$ dB.

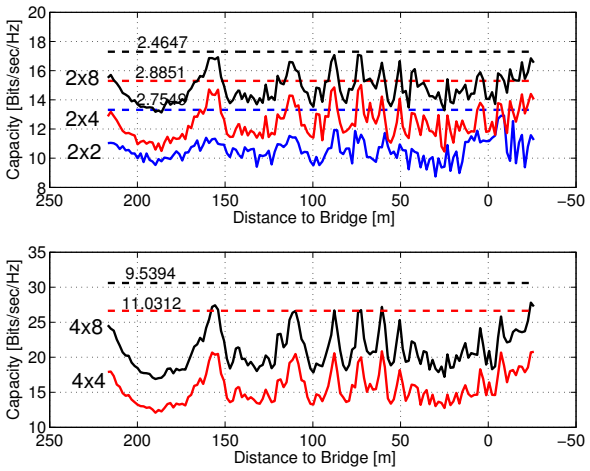

Fig. 5. Capacity versus distance for Small-Small (SS) setup, $\rho = 20$ dB.

from the street surface. In the low pass domain, this two-path channel model can be described as follows,

$$h_T(\tau) = a_1 e^{-j2\pi f_o \tau_1} \delta_T(\tau - \tau_1) + a_2 e^{-j2\pi f_o \tau_2} \delta_T(\tau - \tau_2), \quad (5)$$

where f_o is the center frequency of the transmitted signal and a_1 and a_2 are the amplitude factors for the LOS and reflection paths respectively. They are normalized such that $a_1^2 + a_2^2 = 1$. The dirac function, δ_T, is defined by $\delta_T(\tau) = \delta(\tau) * h_T(\tau)$, where $h_T(\tau)$ is the impulse responce of an ideal lowpass filter. Equation 5 can also be simplified to

$$h_T(\tau) = a_1 \delta_T(\tau) + a_2 e^{-j2\pi f_o \Delta\tau} \delta_T(\tau - \Delta\tau), \quad (6)$$

where τ_1 is assumed to be zero.

A. Coherence Bandwidth

A channel is said to be frequency selective if the bandwidth, BW, of the transmitted signal is much larger than the coherence bandwidth BW_c of the channel, i. e. $BW >> BW_c$. The coherence bandwidth of the channel is defined by $BW_c \approx \frac{1}{\Delta\tau}$, where $\Delta\tau$ is the multipath spread of the channel. In case of a two path channel, it is equal

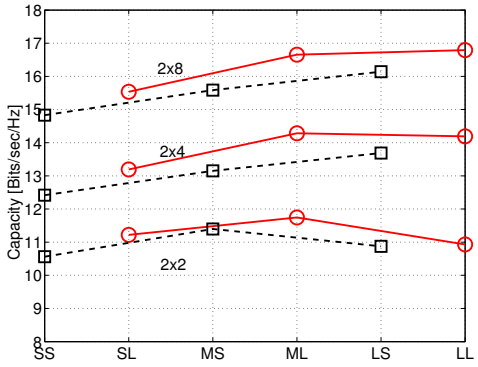

Fig. 6. Mean capacity for MIMO $2 \times n_R$, $\rho = 20\,\text{dB}$.

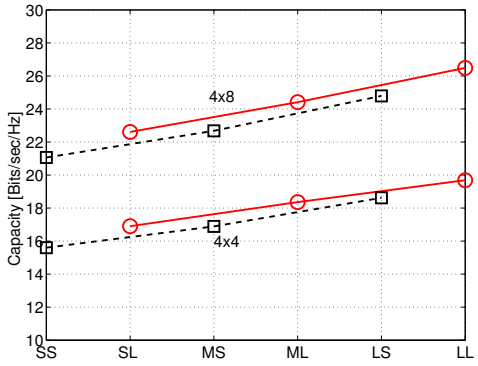

Fig. 7. Mean capacity for MIMO $4 \times n_R$, $\rho = 20\,\text{dB}$.

to the delay difference between the two channel taps. If the delay $\Delta\tau$ is too small, the received signal experiences flat fading. However, for the model considered here, the fading is not random as in a Rayleigh channel, but changes in a predictable fashion as the transmitter approaches the receiver.

B. Channel Model Simulation Results

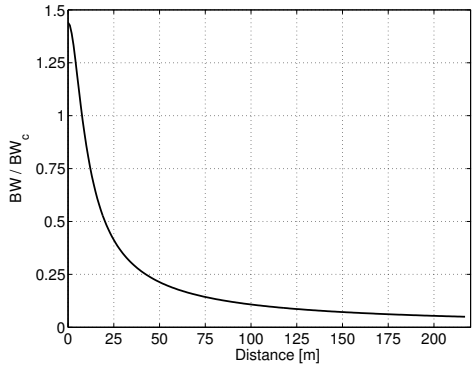

Fig. 8. Ratio of BW to BW_c versus distance between transmitter and receiver.

As mention in Section II, $f_o = 5.2\,\text{GHz}$ and $BW = 120\,\text{MHz}$. These values were also used for the simulations to calculate the delay difference. At large seperations, the delay difference, $\Delta\tau$, is small and increases with decreasing distance between the transmitter and receiver. Figure 8 shows how the ratio $\frac{BW}{BW_c}$ changes with decreasing distance between the transmitter and the receiver. As can be deduced from this figure, the channel remains non-frequency selective expect at very short distances, where $\frac{BW}{BW_c} > 1$. Figure 9 shows a

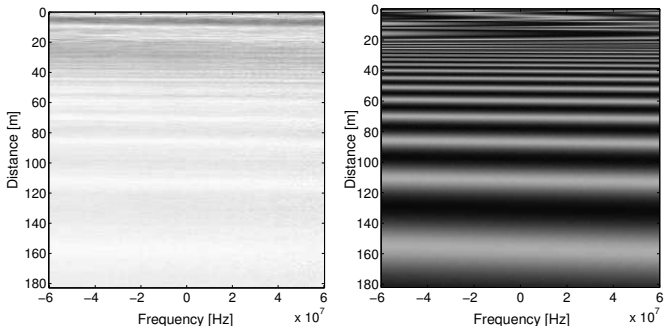

Fig. 9. Spectrogram of measured and simulated two-path channel ($a_1 = a_2$).

spectrogram of a typical measured channel (left) and that of the simulated channel (right). As mention earlier, the amplitude of the simulated two path channel was normalized to 1.0. The measured channel shown was not normalized and thus the difference in the gray intensity of the spectrograms. Apart from that, both spectrograms are quite comparable, which backs the assumed two-path model.

VI. Conclusion

We have looked at the capacity of a real outdoor MIMO channel as a function of array element spacing and distance between transmitter and receiver. We found minor changes in the capacity with decreasing distance between the transmitter and the receiver. Yet, the capactiy was found to increase as the spacing between antenna elements at either the transmitter or the receiver arrays increased. The fluctuations of the capacity as the transmitter approached the receiver were assumed to be due to reflections from the street surface that periodically lead to destructive or constructive interference. A two-path channel model was simulated to back this assumption.

Acknowledgment

The work has been partly supported by following research projects (grant no.): HyEff (01BU156 and 01BU158), WIGWAM (01BU375) by German Ministry of Education and Research (BMBF), IST-WINNER (IST-2003-507581) by European Union and TakeOFDM (Li659/6-1) by German research foundation (DFG). The authors also thank Dr. Wim Kotterman for his helpful discussions.

References

[1] I. Telatar, "Capacity of multi-antenna gaussian channels," *Technical Memorandum, ATT Bell Laboratories, Lucent Technologies*, Oct. 1995.

[2] G. Bauch, *„Turbo-Entzerrung" und Sendeantennen-Diversity mit „Space-Time-Codes" im Mobilfunk*. VDI-Verl., 2001, ISBN: 3-18-366010-5.

[3] R. S. Thomä, D. Hampicke, A. Richter, G. Sommerkorn, and U. Trautwein, "MIMO Vector Channel Sounder Measurement for Smart Antenna System Evaluation," in *European Transactions on Telecommunications ETT*, vol. 12, pp. 427–438, Sept. 2001.

[4] D. Gesbert, H. Bölcskei, D. Gore, and A. Paulraj, "Outdoor MIMO Wirless Channels: Models and Performance Prediction," *IEEE Trans. Communications*, vol. 50, pp. 1926–1934, Dec. 2002.

[5] D. Yacoub, W. G. Teich, and J. Lindner, "Capacity of Vehicle-Bridge Channel Model," in *Proc. COST 273, 5th Management Committee Meeting, TD(02)118*, (Lisbon/Portugal), Sept. 2002.